Coolant Pressurization and Expulsion for Transpiration Nosetips

THEODORE E. WARD* AND JOHN R. SCHUSTER*
McDonnell Douglas Astronautics Company, Huntington Beach, Calif.

Active transpiration cooling can provide shape stability for re-entry vehicle nosetips. This paper examines the design and performance requirements of positive expulsion systems required to supply liquid coolant to the nosetip, and presents the results of a comprehensive analytical and experimental program that evaluated bladder and piston expulsion systems pressurized by unvented solid propellant warm gas generators. Stable, predictable pressurization was obtained up to 8000 psi and 200 g's, and conical elastomeric bladders were found to yield high expulsion efficiencies while providing good thermal insulation between the hot gas and the coolant.

Introduction

ADVANCED re-entry vehicles, both ballistic and maneuvering, will require shape-stable nosetips in order to meet proposed targeting objectives. For passive materials acceptable nosetip designs may not be feasible, particularly if the vehicle is expected to pass through an erosive, particle-laden environment. A transpiration-cooled nosetip (TCNT) shows promise of providing the required shape stability, and it has been successfully demonstrated, both during ground and flight tests.

The components of the TCNT coolant supply system are undergoing systematic development to make them compatible with the requirements of advanced vehicles. These requirements include a light weight compact design, long term storage capability, and enough performance flexibility to satisfy a variety of re-entry missions. Figure 1 illustrates the main elements of a TCNT system. In addition to the nosetip, the system includes a valve to vary the flow of liquid coolant, a reservoir for coolant storage, and positive expulsion during re-entry, and a pressure source that can force the coolant through the nosetip against the high external pressure. This system must be packaged in a conical volume directly behind the nosetip.

The present paper establishes coolant supply system flow and pressure requirements for several re-entry missions. The details are presented of a development program that was conducted to provide an experimental evaluation of elastomeric coolant expulsion bladders pressurized by unvented solid propellant gas generators. These components represent design approaches recommended for future TCNT systems.

Nosetip Coolant Requirements

The basic approach generally used to analyze transpiration cooling is to decouple the porous matrix flow and boundary-layer flow. This is done by assuming surface temperature distributions and boundary-layer similarity such that thermally ideal coolant flux distributions can be evaluated for the heated surface. The porous structure is then designed such that its hydraulic characteristics result is an actual coolant distribution that closely matches the thermally ideal distribution.

Schuster and Lee[1] provide details on the calculation of ideal coolant flux, and Schuster and Seay[2] describe techniques for calculating the actual three-dimensional coolant distribution within transpiration cooled nosetips. Utilizing these methods, a nosetip design was evolved for a high ballistic coefficient re-entry vehicle that was postulated to have multimission capability. Liquid water, which has a high heat absorption capacity, was selected as the coolant. For this nosetip Fig. 2 presents the required coolant flow and Fig. 3 the associated coolant pressure for a family of five different re-entry trajectories. Sharp changes in the flow and pressure are due to variations in the angle of attack of the re-entry vehicle. As can be seen, the coolant flow histories vary substantially among these five trajectories. Table 1 presents a summary of coolant requirements. It should be emphasized that these represent conditions that must be provided by the flow control valve component shown in Fig. 1.

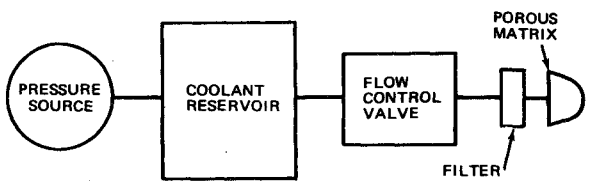

Fig. 1 Transpiration system components.

The coolant weights in Table 1 were calculated assuming a coolant temperature of 530°R. Figure 4 presents the coolant weight for trajectory 1 as a function of coolant temperature. Coolant viscosity decreases with increasing temperature, resulting in greater streamline curvature of the coolant flow within the isotropic porous nosetip material. Streamline curvature is caused

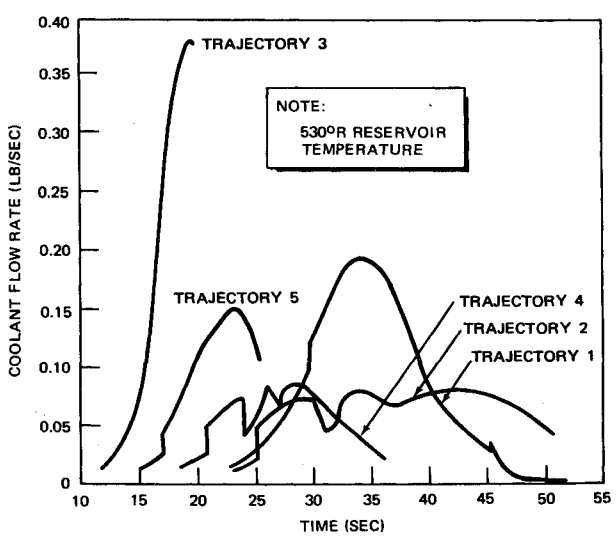

Fig. 2 Coolant flow histories.

Presented as Paper 73-1231 at the AIAA/SAE 9th Propulsion Conference, Las Vegas, Nev., November 5–7, 1973; submitted November 5, 1973; revision received March 11, 1974. This work was supported by McDonnell Douglas independent research and development funds.

Index categories: LV/M Propulsion System Integration; Thermal Modeling and Experimental Thermal Simulation; Thermal Surface Properties.

* Research Engineering Scientist.

Table 1 Nosetip coolant requirement summary

Trajectory	Coolant total weight (lb)	Peak flow (lb/sec)	Peak pressure (psia)
1	2.31	0.193	3036
2	1.81	0.0813	1280
3	1.30	0.378	6317
4	0.982	0.0867	1378
5	0.962	0.150	2375

by the external tangential pressure gradient being transmitted into the porous material and interacting with the radial pressure field. In view of the trend of Fig. 4 it is desirable to prevent coolant temperature heating from occurring in the storage reservoir.

Coolant Flow Control

In order to proportion coolant flow to meet nosetip thermal requirements, either the pressurant gas or the liquid coolant can be modulated. Practical design problems result in coolant modulation being the most attractive option. In addition, the required coolant flow histories of Fig. 2 and the coolant pressure histories of Fig. 3 are compatible, therefore providing the option of modulating either coolant flow or coolant pressure at the outlet of the control valve. Since there are uncertainties in the evaluation of the pressure required to achieve a desired flow, and coolant flow is the essential quantity preventing nosetip failure, then direct modulation of coolant flow rate is the most reliable control approach. In order to minimize complexity, the valve should be kept as simple as possible.

Figure 5 presents a functional schematic of a developed and proven mechanical valve with one moving part that controls coolant flow by utilizing the deceleration of the re-entry vehicle. The valve holds a differential pressure, which is a function of deceleration, across a fixed orifice. The force due to deceleration of the ballast mass on the end of the spool is opposed by a pressure imbalance across the spool. This pressure imbalance is caused by the pressure drop as the coolant flows through the fixed orifice. When there is a net force imbalance, the spool moves, causing the variable orifice size to change, therefore changing flow rate. In this way the valve compensates for changes in upstream and downstream pressure, providing a flow rate that is a function of deceleration. As deceleration is directly related to aerodynamic heating, there is a good correlation with required coolant flow. The valve will provide a deceleration dependent flow rate, regardless of upstream and downstream pressures, as long as there is sufficient upstream pressure.

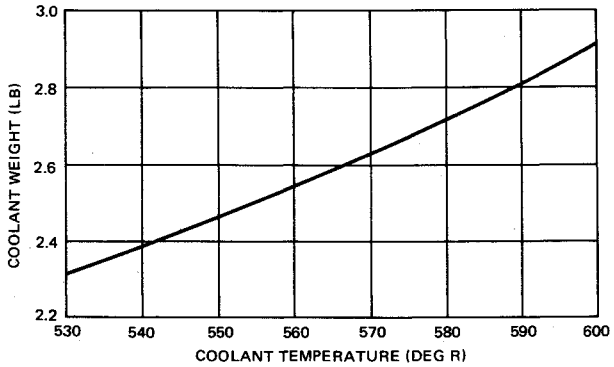

Fig. 4 Effect of coolant temperature on coolant weight.

Pressurization Concepts

As can be seen from Fig. 3, the pressure required for coolant expulsion is a function of time and the specific re-entry trajectory. Fortunately, the TCNT valve design regulates coolant flow independent of upstream pressure and any pressure greater than the minimum required for adequate flow is acceptable.

Cold gas blowdown, solid propellant gas generators, and bootstrap and blowdown monopropellant gas generators can be applied to this oroblem. The complication of a bipropellant concept is not warranted.

Cold Gas Pressurization

Cold gas helium pressurization has been used on previous test flights of TCNT systems. Maximum storage pressure has been 10,000 psi. Blowdown analyses of the flow and pressure histories shown in Figs. 2 and 3 result in the helium bottle weight and volume relationships shown in Fig. 6.

The optimum gas storage pressure would be between 20,000 psi and 30,000 psi, which is higher than normally used in blowdown applications. However, this pressurization technique is well established, and development costs should be lower than for other methods. Disadvantages of cold gas pressurization are subsystem size, storage, safety, and handling. With 20,000 psi gas pressure, the subsystems are still substantially larger than most warm gas pressurization concepts.

Warm Gas Pressurization

Pressurization of the coolant by combustion products of propellants is very attractive because of the small volume needed for storage of the solid or liquid propellant. If size were not critical, it would be questionable whether warm gas subsystems

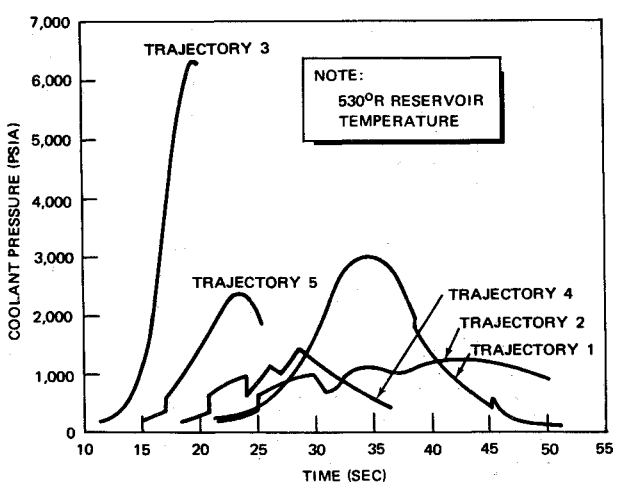

Fig. 3 Coolant pressure histories.

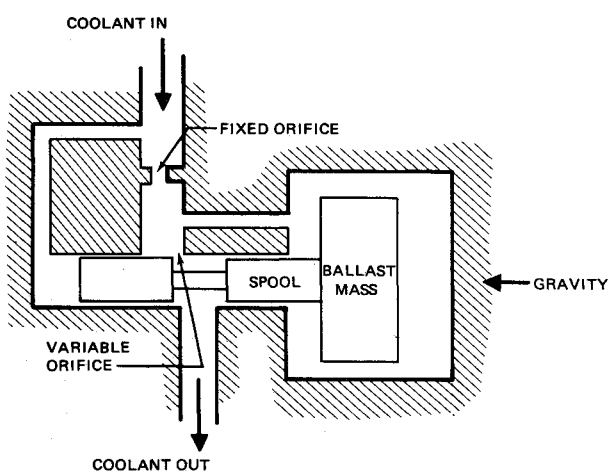

Fig. 5 g-sensing flow control valve.

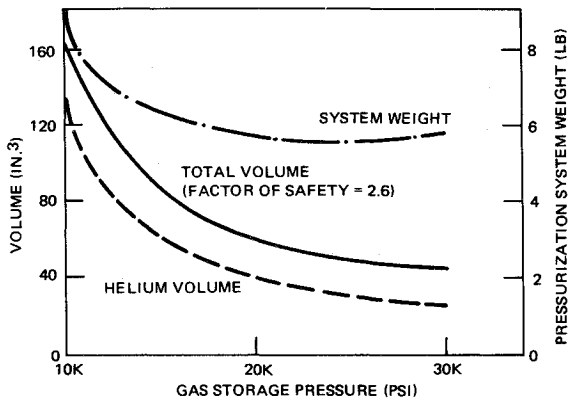

Fig. 6 Helium gas bottle volume and weight.

should be used in TCNT applications as there are numerous problems associated with pressure control and thermal effects that are not present with cold gas pressurization. In particular, the gas generator performance and design is complicated by the requirement that it be nonventing. Integration of the TCNT system into the re-entry vehicle does not permit room for ducting vent gases aft so that they can be exhausted out the vehicle base heat shield. Venting the gases through the forward heat shield would cause considerable thermal problems and would have an adverse effect on vehicle stability and control.

Solid propellant gas generators

Referring to Figs. 2 and 3, high presure levels are required for short trajectories with high flow rates; i.e., high pressures must be achieved early and after large amounts of coolant have been expelled. Long trajectories are just the opposite; pressure requirements are low with little coolant expelled for several seconds.

It can be seen that to avoid high design pressures, single grain designs require large ullage volumes for multiple trajectory applications. Two grains, with the second ignited by a trajectory dependent function, have been found to reduce the gas generator size by more than one half. Very little additional reduction in size is obtained by going to designs with three or more grains because grain geometry and the requirement for additional insulation around the propellant offset the reduction in ullage volume. In addition the complexity of signaling for ignition of additional grains reduces reliability.

The signal to ignite the second grain may originate at a sensor that measures 1) pressure in the gas generator; 2) time after ignition of the first grain; 3) acceleration level; or 4) pressure drop across the valve. The first three have been found to require larger ullage volumes for operation than the fourth, which senses when flow is becoming inadequate.

Monopropellant gas generators

Monopropellant gas generators are attractive for pressurization of the TCNT system because of the "on demand" operation available in liquid systems. With this concept, propellant flow to a catalyst bed can be controlled by a pressure sensitive flow valve. Gas generation can therefore be terminated at a pressure level that adequately pressurizes all trajectories, and be restarted when pressure drops below the design level. Furthermore, the temperatures of the gases can be controlled with catalyst bed geometry to be as low as necessary to reduce heat transfer to the coolant reservoir.

There are disadvantages with monopropellant concepts when compared with solid propellant gas generators. Monopropellant concepts are larger. This is related to the need for a larger fuel volume because of lower fuel density, and less energy released by monopropellant decomposition. There are also disadvantages associated with a more complex design. Long-term storage is more of a problem with monopropellants than with solid propellants.

Two types of monopropellant pressurization concepts were considered for TCNT system applications. Both a blowdown stored gas concept and a bootstrap or differential area piston concept could be adapted to the TCNT gas generator requirements. The bootstrap monopropellant concept appears to be more compact.

Coolant Expulsion Concepts

Both bladder and piston reservoirs can be used for expulsion of the coolant. Although piston expulsion concepts have been used on previous flight tests and have few development problems, pistons must move within cylindrical chambers, and do not efficiently use a conical volume. In contrast, bladders have a high volumetric efficiency in a conical coolant chamber.

An elastomeric bladder is very attractive for TCNT flight systems. In comparison with metallic bladders, elastomeric bladders have the advantage of lower cost, and they can be prechecked by cycling them with cold gas. Elastomeric materials also have low thermal conductivity, permitting less heat to be transferred into the coolant when using a warm gas generator for pressurization. As indicated in Fig. 4, heat transfer can have a significant effect on the amount of coolant required. The material, however, must survive gas temperatures which can be initially in excess of 2,000°F. Chemical reaction of the propellant gases with the elastomeric material is possible. In general, the environmental limits that a bladder can withstand are hard to define due to transient operating conditions.

Pressurization Analysis

In order to aid design, a computer program was developed to study the transient performance of unvented pressurization/expulsion subsystems. The capability of the program includes cold gas, solid propellant or monopropellant warm gas generators, piston or bladder expulsion systems, and various flow control techniques. The program allows numerous design options to be inserted into the analysis and provides a substantial quantity of data for preliminary design. Printouts of graphs and tables are generated to describe the behavior of important variables.

An Euler method of numerical integration was selected to describe the system operation with extensive heat and mass transfer within closed boundaries. The heat transfer model includes a 600 unit axisymmetric heat transfer structure so as to calculate temperatures at 10 radial locations and 60 axial locations in a cylindrical or conical wall with variations in matrix materials and axial geometry.

The gas generation computations describe the combustion of the solid propellant or decomposition of a monopropellant, with allowance for the effects of mass addition, phase changes, heat losses, and fluid displacement on pressure. Fluid displacement is based on either calculations of fluid flow through an orifice, numerical simulation of flow through a valve as a function of a flight variable, or an independent flow history. Gas temperatures are calculated from an integrated total enthalpy value which accounts for axial variations, heat addition by entering mass, heat flux to the walls of the chamber, and work done in expelling the fluid. Temperature distributions are computed for gas segments that divide the chamber axially into units that correspond with divisions of the wall. Compositions of a gas node are determined with a mixing model frequently used for well mixed continuous flow systems. Heat transfer coefficients are obtained from a Nusselt number derived from a function of Grashof and Prandtl numbers. This method allows for the effect of acceleration on heat transfer.

The solid propellant combustion model includes provision for ignition, flame spreading, acceleration effects, irregular burning due to quenching or heating of the grain, variable web, multiple

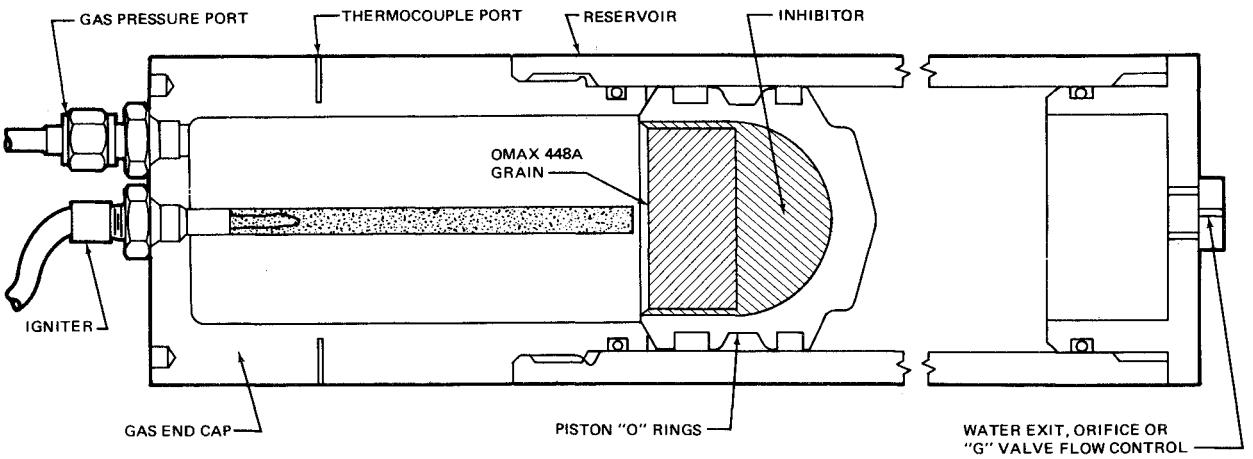

Fig. 7 Single grain/piston reservoir.

grains with different igniters and ignition times, and propellants with complicated burn rate-pressure relationships. The monopropellant decomposition model includes provisions for a pressure sensitive control of flow to the catalyst bed, bed geometry effects on product composition and temperature, and catalyst differences.

Because the solid propellant exhaust gases contain a substantial amount of water vapor, it was found that the analytical model also had to include a description of condensation on the walls of the pressure vessel. Condensation is not normally observed in vented gas generators, but pressure in the unvented gas generator is significantly affected by mass changing phase.

Test Program

An extensive test program was conducted to evaluate the performance of invented solid propellant gas generators in conjunction with piston and elastomeric bladder reservoirs. Gas pressures up to 8,000 psi and acceleration levels to 220 g's were investigated.

Single Grain/Piston Reservoirs

Figure 7 illustrates a piston reservoir expulsion system that was constructed to provide information on the effects of initial ullage volume, coolant flow rate, and lateral or axial acceleration on gas generator performance. References 3 and 4 provide detailed descriptions of these tests. The cylindrical reservoir was capable of holding 3.4 lb of water, had a 2.875 in. diam piston, and was used with various end cap gas ullage chambers that had igniter and instrumentation mountings. The propellant grain and inhibitor were mounted inside the floating piston. This allowed a grain diameter of 2 in. with a $\frac{1}{16}$ in. thick insulation. A warm gas ammonium nitrate solid propellant, OMAX 448A, was used in these tests. Water was used as the coolant with the flow being controlled by either a fixed orifice, or by a "g" valve which provided a flow rate proportional to the square root of axial acceleration. The results of these tests provided substantial insight into the problems of operating a solid propellant gas generator within a slowly expanding chamber without venting excess gases.

An attempt to match the analytical and experimental results of 1-g static tests was not immediately successful. It appeared that heat transfer was several times greater than that calculated for normal free convection. Further investigation showed that condensation could be occurring on the chamber walls. The surface of the chamber walls was remaining below 300°F, pressures were in excess of the critical pressure, and the propellant combustion products contained a substantial amount of water vapor. Since condensation affects the system by reducing the mass of gas and resulting pressure, and also increasing heat transfer to the wall, the amount of condensation remained to be determined.

It was recognized that a finite time is required for transport of the water vapor from the flame zone to the chamber wall and that some amount of water vapor will remain in the gas when equilibrium between the gas and wall is established. The amount remaining in the gas was determined from the partial pressure of water vapor at the average surface temperature of the wall. Figure 8 shows the results of using a transport time of 1 sec.

When the pressurization system was subjected to axial acceleration, an additional effect of condensation was discovered. Water vapor condensing on the walls of the gas chamber ran along the walls in the direction of the acceleration vector. This happened to be towards the piston and the cup containing the grain. When a sufficient amount of condensate reached the burning grain (in 2 to 3 sec), the grain was extinguished.

One simple solution to this problem was tried with adequate results. A sleeve was placed around the grain so that condensate would be trapped between the sleeve and the walls of the chamber. The maximum amount of condensate was known, and the annulus formed between the sleeve and wall was sized to contain this amount. The material used for the sleeve was found to be important. The successful design used a sleeve made of glass phenolic. A steel sleeve was not successful. Condensation apparently occurred on the metal sleeve and the propellant was quenched before combustion could be completed.

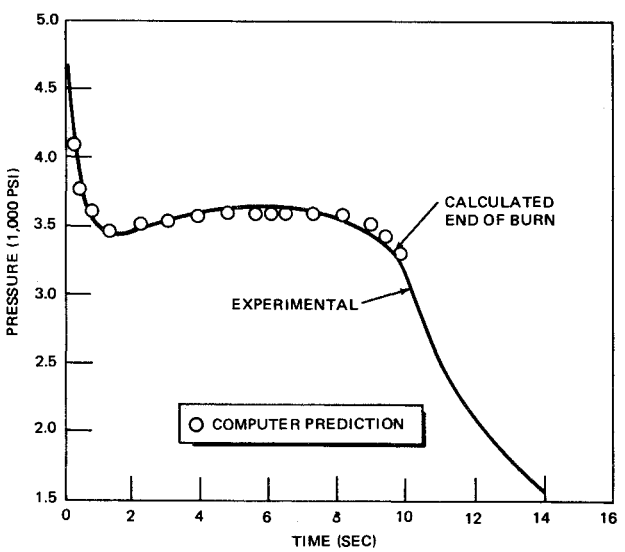

Fig. 8 Pressure history for static test.

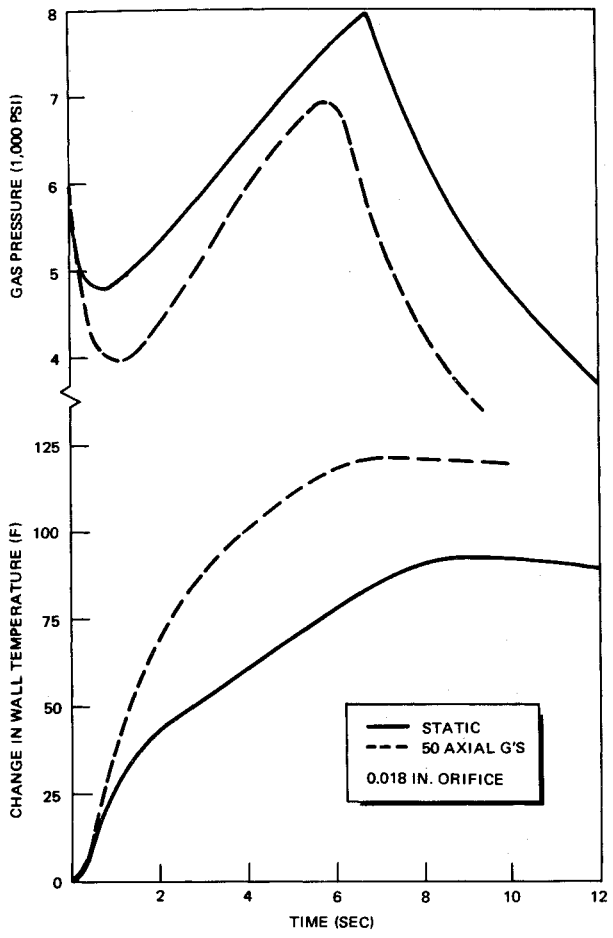

Fig. 9 Effect of acceleration on pressurization system.

Another effect of acceleration is that heat transfer is increased. For natural convection, the increase in heat transfer coefficient is proportional to g's raised to a power. This power was assumed to vary between 0.25 and 0.40 according to the magnitude of the Grashof and Reynolds numbers. For the system tested, the increase in heat transfer due to acceleration is illustrated in Fig. 9. The acceleration causes an increase in heat transfer to the walls of the chamber, which reduces the gas temperature causing a reduction in chamber pressure. Temperatures in the chamber wall reflect the increase in heat transfer, showing approximately 30% greater rise in temperature when the system was tested at 50 g's.

The temperature rise is not proportional to the increase in heat transfer coefficient for two reasons: 1) the greatest part of heat transfer to the wall is through condensation which is not appreciably affected by acceleration (other than movement of the condensate; and 2) the system is approaching thermal equilibrium at the end of burn. Calculations made with the computer program, which allows for condensation and gas temperature variation, have shown that an increase in heat transfer coefficient by g's to the 0.4 power is a good description of convective heat transfer within the system under acceleration.

Table 2 Bladder material combinations and properties

	Material specimen 1	2	3	4	5
Fabric:					
Nomex	X			X	
Quartz	X	X			X
PBI		X	X	X	X
wire/asbestos			X		X
Rubber:					
Silicon (red)	XX		X (water side)		
Flurocarbon (BN)		XX	X (gas side)	XXX	XX
Vapor dep. metal					X (gas side)
Density lb/ft^3	85.4	116.1	92.1	110.0	98.6
Specific heat B/lb°F					
70°F	0.255	0.235	0.195	0.220	0.190
250°F	0.324	0.327	0.252	0.229	0.301
Conductivity B/ft°F hr					
130°F	0.139	0.093	0.097	0.089	0.116
170°F	0.134	0.092	0.097	0.089	0.113
260°F	0.125	0.087	0.093	0.086	0.110
Water absorption	L	H	M	H	H

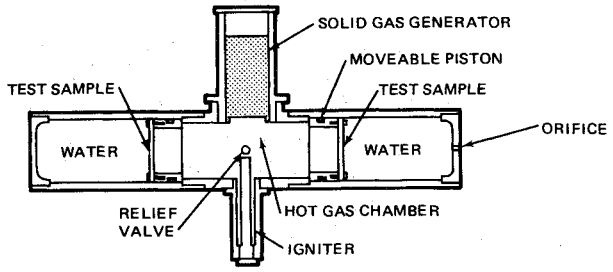

Fig. 10 Bladder material test fixture.

Elastomeric Material Evaluation

Prior to fabricating full-scale elastomeric bladders a study was conducted to evaluate the performance characteristics of candidate materials. Four types of fabric and two types of rubber were considered, as well as a vapor deposited metallic film. Table 2 summarizes the fabric/rubber material combinations for the five samples that were fabricated and also presents experimental values for their thermophysical properties. Also shown are the results of water absorption tests that were performed.

Two piston reservoirs were modified to produce the bladder material test fixture shown in Fig. 10. The reservoir contained two annular pistons, each with a sample diaphragm of bladder material held in place. Both ends of the reservoir contained water, but one end had an orifice to allow coolant expulsion while the other end was stagnant, permitting a thermocouple to be attached to the water side of the bladder material. Gas generator temperature and pressure were also measured. Table 3 presents the results of the tests.

From the standpoint of thermochemical performance in the hot gas environment, all the materials were adequate.

Dual Grain/Bladder Reservoirs

Based upon the encouraging results of the single grain/piston reservoir tests and the elastomeric material tests, full-scale elastomeric bladders and dual-grain solid propellant gas generators were made and several tests conducted using the configuration shown in Fig. 11. Reference 5 provides details on these tests.

Table 3 Bladder material test results

Test parameter	Material specimen 1	2	3	4	5
Time, sec	35	36	41	34	38
Peak press, PSI	2940	3700	2520	3600	3450
Peak temp °F	950	620	832	780	728
Diaphragm temp. rise °F	228	112	...	80	160
Material loss	slight	mod.	none	mod.	none

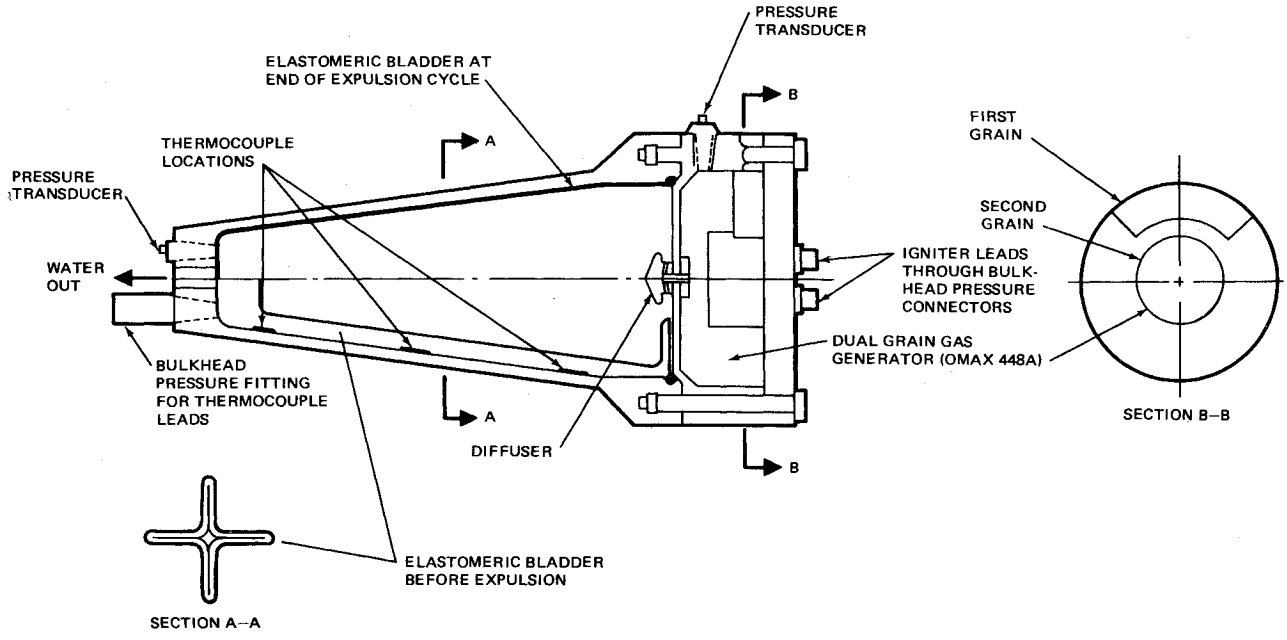

Fig. 11 Test reservoir with cruciform elastomeric bladder and dual grain gas generator.

The dual grain solid propellant gas generator closely resembled a possible flight design. A 90° circumferential-burning first grain was used to provide up to 30 sec of low level pressurization as would be required during early stages of re-entry. A 2.5 in. diameter end-burning grain was ignited after several seconds to demonstrate that high level pressurization could be obtained if required during peak re-entry heating of the TCNT. The gas generator was completely contained in a 2 in. × 5.25 in. diam cylinder. The second grain was insulated by a fiberglass cap which was separated by a package igniter placed between the insulation and grain surface. Gas flowed from the gas generator through a 0.25 in. diffuser into the elastomeric bladder which expelled up to 4.5 lb of water through a 0.021 in. orifice.

The bladder was of cruciform design with the water being contained between the outside of the bladder and the reservoir walls. It is not clear that a cruciform design is better than other possible configurations. However, it avoids rolling of the bladder material along the walls, which could cause delamination of the elastomer from the fabric, and also provides high expulsion efficiency. Cold gas expulsion tests showed the bladder to yield 99% expulsion efficiency while pressurized at 100 psi in both one "g" and 200 g's acceleration applied perpendicular to the bladder axis.

Two types of composite were used to fabricate bladders with a 60 mil average wall thickness. One type was Butyl rubber covering nylon cloth and the second type was Viton rubber covering PBI cloth. Both combinations resulted in good strike through and adhesion to the cloth fabric.

Several static and 200 g centrifuge tests were conducted and it was demonstrated that the dual grain solid propellant gas generator adequately pressurized the coolant in an environment representative of re-entry conditions.

Modifications had to be made to the package containing the second grain, as premature ignition of that grain occurred for the first static test and also for the first 200 g acceleration test. The final design employed a fiberglass cup containing the grain with a steel case around the fiberglass to resist the 200 g lateral acceleration. This approach was simple, adequate, and compact, but it is apparent that precautions are necessary to ensure that insulation package is properly sealed after fabrication. A larger number of tests would be required to develop confidence in the design and to establish reliability, but no major problems in developing a flight design with this concept are anticipated.

Modifications also had to be made to the diffuser design. During the first 200 g test the bladder folded up against an outlet in the diffuser which directed a flow of high-velocity gas directly against the material. As a consequence the bladder was perforated near the end of the 30 second test. The diffuser was redesigned with a shield over the outlet and the subsequent test yielded no problems.

Figure 12 presents a composite of results from two static tests along with the pretest computer prediction and also a 200 g test. The two static tests differed in that one ignited only the first grain while the other ignited both grains. Very close agreement between the two tests is apparent for the first 20 seconds indicating that the concept offers repeatability. The computer prediction also compares very well with the test results. As occurred for the single grain/piston reservoir tests, pressures were reduced due to acceleration. Acceleration effects on heat transfer to the case reduced peak pressure from 5,500 psi to 4,500 psi.

The feasibility of this pressurization system has been demonstrated in these tests, but numerous questions still remain con-

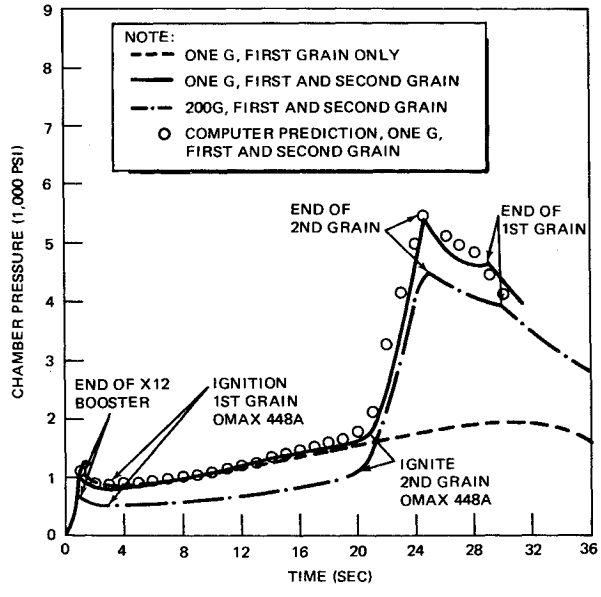

Fig. 12 Dual grain gas generator pressurization histories.

cerning operation under multiple trajectory applications with control valves to limit coolant flow. In general, both the Viton-PBI and Butyl-nylon bladders were only slightly damaged under exposure to solid propellant combustion gases, and were re-used in some cases without failure. The coolant side of the bladder was generally unchanged after testing. The lifetime of elastomeric bladders in this environment is apparently quite extensive. With the elastomeric bladder thicknesses used in these tests, there is very little increase in coolant temperature as indicated in Table 4, and heat transfer to the coolant definitely does not appear to be an important problem when low conductivity elastomeric materials are used.

Improvement in bladder technology is considered possible in several areas, including materials, bladder designs, fabrication techniques, and pretest examination methods. Based on the experimental data gathered in these tests, and the low cost and high volumetric efficiency of an elastomeric bladder, elastomeric bladder expulsion concepts for TCNT appear to be very attractive.

Table 4 Coolant temperature increase during test

G level	Maximum pressure (psig)	Duration (sec)	Coolant temperature rise (°F)
1	7000	21	9
1	7000	23	5
1	4700	30	7
1	2200	36	13
1	5450	180	27
200	5100	40	31[a]
200	4500	40	9

[a] Bladder perforated.

Conclusions

From the discussion and test results the following conclusions are presented concerning the application of solid propellant gas generators and elastomeric coolant bladders to TCNT systems.

1) Unvented solid propellant gas generators provide stable, repeatable pressurization for both piston and bladder reservoirs up to 8,000 psi and 200 g's.

2) The effect of acceleration is to reduce the level of pressurization because of increased heat transfer to the walls of the chamber.

3) The heat transfer in the unvented chamber can be correlated assuming natural convection with a heat transfer coefficient proportional to the g-level raised to the 0.4 power and by accounting for energy transfer to the walls of the chamber due to condensation.

4) The lifetime of cruciform elastomeric bladders in the hot gas environment is considerably longer than required for expulsion of coolant to a transpiration nosetip during re-entry.

5) The elastomeric bladder yields high expulsion efficiency, even under 200 g's acceleration perpendicular to the bladder axis.

6) The elastomeric bladder provides good thermal insulation between the hot gas and coolant.

References

[1] Schuster, J. R. and Lee, T. G., "Application of an Improved Transpiration Cooling Concept to Space Shuttle Type Vehicles," *Journal of Spacecraft and Rockets*, Vol. 9, No. 11, Nov. 1972, pp. 804–811.

[2] Schuster, J. R. and Seay, G. E., "Simulation of Three-Dimensional Coolant Flow Within Transpiration Nosetips," presented at the 7th AIAA/NASA/ASTM/IES Space Simulation Conference, Los Angeles, Calif., Nov. 1973.

[3] Ward, T. E., "Testing and Analysis of Solid Propellant Pressurization/Expulsion Systems," MDAC Rept. G 2638, Dec. 1971, McDonnell Douglas Astronautics Co., Huntington Beach, Calif.

[4] Glickman, R. A. and Ward, T. E., "Hot Gas Expulsion System Test Program," MDAC Rept. G 2601, Feb. 1972, McDonnell Douglas Astronautics Co., Huntington Beach, Calif.

[5] Ward, T. E., "A Pressurization Expulsion System for Transpiration Cooled Nosetips (TCNT)," MDAC Rept. G 4848, Sept. 1972, McDonnell Douglas Astronautics Co., Huntington Beach, Calif.